Proc. Natl. Acad. Sci. USA
Vol. 88, pp. 11207–11211, December 1991
Biophysics

Rapid-flow resonance Raman spectroscopy of bacterial photosynthetic reaction centers

(electron transfer/hole-burning spectroscopy/excited-state dynamics/resonance Raman intensities)

ANDREW P. SHREVE*, NERINE J. CHEREPY*, STEFAN FRANZEN†, STEVEN G. BOXER†‡, AND RICHARD A. MATHIES*‡

*Department of Chemistry, University of California, Berkeley, CA 94720; and †Department of Chemistry, Stanford University, Stanford, CA 94305

Communicated by Lubert Stryer, September 4, 1991 (received for review July 28, 1991)

ABSTRACT **Rapid-flow resonance Raman vibrational spectra of bacterial photosynthetic reaction centers from the R-26 mutant of *Rhodobacter sphaeroides* have been obtained by using excitation wavelengths (810–910 nm) resonant with the lowest energy, photochemically active electronic absorption. The technique of shifted excitation Raman difference spectroscopy is used to identify genuine Raman scattering bands in the presence of a large fluorescence background. The comparison of spectra obtained from untreated reaction centers and from reaction centers treated with the oxidant $K_3Fe(CN)_6$ demonstrates that resonance enhancement is obtained from the special pair. Relatively strong Raman scattering is observed for special pair vibrations with frequencies of 36, 94, 127, 202, 730, and 898 cm^{-1}; other modes are observed at 71, 337, and 685 cm^{-1}. Qualitative Raman excitation profiles are reported for some of the strong modes, and resonance enhancement is observed to occur throughout the near-IR absorption band of the special pair. These Raman data determine which vibrations are coupled to the optical absorption in the special pair and, thus, probe the nuclear motion that occurs after electronic excitation. Implications for the interpretation of previous hole-burning experiments and for the excited-state dynamics and photochemistry of reaction centers are discussed.**

Bacterial photosynthetic reaction centers (RCs) are the pigment–protein complexes in which the light-induced charge-separation reactions of photosynthesis occur (1–4). The primary electron donor is a dimer of bacteriochlorophyll (Bchl) molecules called the special pair (P). After optical excitation, electron transfer from ^1P, the lowest-energy singlet excited electronic state of P, to a bacteriopheophytin acceptor occurs within about 3 ps at room temperature. Electroabsorption measurements suggest that ^1P contains a large amount of charge-transfer character (4–8), and hole-burning studies and theoretical models indicate that strong coupling exists between electronic and vibrational motions in P (9–20). The electronic–nuclear coupling determines the nuclear motion that occurs after electronic excitation, but the description of this motion, including its role in possibly mediating the primary charge transfer, has been hampered by the lack of information about the vibrational modes of P that are coupled to optical excitation.

Resonance Raman spectroscopy can provide information necessary to address many of the unresolved questions about the electronic and vibrational dynamics of RCs. The vibrational modes that appear in a resonance Raman spectrum are just those modes that are coupled to the optical excitation (21), so the ground electronic state frequencies of the coupled modes are determined. In addition, quantitative analysis of the resonance Raman intensities and assignment of the resonance Raman-active modes can provide a picture of the nuclear distortions that occur upon electronic excitation (21). Because these distortions reflect the underlying excited electronic state potential energy surface, resonance Raman studies of photochemically active systems, like photosynthetic RCs, can probe the role of nuclear motions in the photochemical reaction.

Resonance Raman with excitation into the lowest energy absorption band of RCs (see Fig. 1) is challenging, because of both intrinsic photochemical bleaching of P and interference from RC fluorescence. The first difficulty can be avoided by use of the rapid-flow technique (22), but even if all sources of impurity fluorescence are removed, the intrinsic fluorescence of RCs has a quantum yield of $\approx 4 \times 10^{-4}$ (23) and is much larger than the Raman scattering (see below). To overcome this problem and identify genuine Raman bands, we use shifted excitation difference spectroscopy. In this technique, the difference is taken of two emission spectra obtained with excitation frequencies differing by a few wavenumbers. The fluorescence background is essentially unaffected by the shift in excitation frequency and, thus, disappears in the difference spectrum, leaving only a Raman difference spectrum. This technique has been successfully used to obtain resonance Raman spectra of bacterial RCs, and a variety of control experiments has been done to show that the observed lines result from resonance enhancement by P.

MATERIALS AND METHODS

RCs were isolated from *Rhodobacter sphaeroides* (R-26), and the secondary quinone electron acceptor (Q_B) was depleted according to established procedures (24, 25). RCs were solubilized in 10 mM Tris/0.025% lauryldimethylamine-*N*-oxide, pH 8.0. The sample concentrations were adjusted to obtain an absorbance at 850 nm of 0.2 to 0.3 in a 1-mm path length. The sample was held at ≈5°C by an ice bath and was circulated through a 1.0-mm (i.d.) square capillary with a linear flow velocity of 200 cm/s. Absorption spectra of aliquots withdrawn periodically showed the samples to be stable for at least a full day under the experimental conditions. For the experiments using oxidized RCs, ≈30 mM $K_3Fe(CN)_6$ was added to an RC sample.

The excitation source was a Ti-sapphire laser (Spectra Physics, model 3900/S) pumped by an argon ion laser (Spectra Physics, model 2020). A 75-mm lens focused the laser beam to illuminate an $\approx 10^{-4}$-cm^2 area of the sample, and the emission was collected in a standard 90° arrangement. The combined Raman and fluorescence emission depended linearly upon the excitation power at the intensities used, and

The publication costs of this article were defrayed in part by page charge payment. This article must therefore be hereby marked "*advertisement*" in accordance with 18 U.S.C. §1734 solely to indicate this fact.

Abbreviations: RC, reaction center; P, special pair; ^1P, lowest-energy singlet excited electronic state of P; Bchl, bacteriochlorophyll; FT, Fourier transform.

‡To whom reprint requests should be addressed.

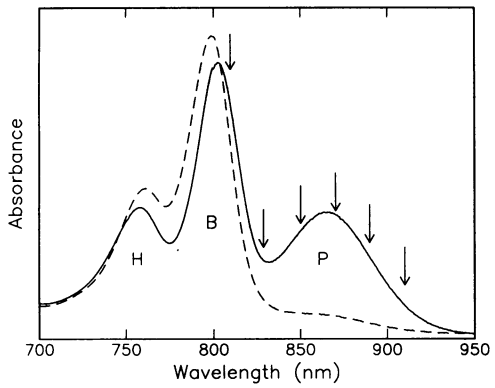

FIG. 1. The near-IR absorption spectra of *R. sphaeroides* (R-26) RCs at room temperature before (——) and after (– – –) treatment with excess $K_3Fe(CN)_6$. Excitation wavelengths (810, 830, 850, 870, 890, and 910 nm) used in this work are indicated by arrows. The labels P, B, and H indicate the absorption bands corresponding to the special pair, monomeric Bchls, and bacteriopheophytins, respectively.

the Raman spectra were unchanged, except in magnitude, by a factor of four decrease in excitation power. A typical excitation power was 0.9 mW at 850 nm; more or less power was used at other wavelengths to achieve the same photoalteration parameter (22). The fraction of RCs excited upon each pass through the laser beam was estimated to be approximately one-third. The emission collected from the sample was focused into a 0.75 M double spectrograph with an entrance slit set for ≈ 8 cm^{-1} resolution. The detector was a charge-coupled device (Princeton Instruments, model CCD/LN) operated at −100°C. The overall spectral sensitivity of the collection and detection apparatus was corrected by using a standard lamp. Because of the breadth of the Raman lines and inherent uncertainty in calibration of the frequency axis, the uncertainties in the reported Raman frequencies are about ± 3 cm^{-1}. Typical accumulation times were 20–40 min.

To overcome the fluorescence background problem, a shifted excitation difference technique was developed. Two emission spectra were obtained with the laser frequency slightly shifted in one relative to the other but with everything else identical, and then the difference of these spectra was taken. In all data reported here, the shift of excitation frequencies was 10 cm^{-1}, but data obtained with shifts of 15 cm^{-1} and 25 cm^{-1} yielded similar results. In all cases, the difference data are reported as shifted minus unshifted excitation, with the spectral axis corresponding to a Raman shift from the unshifted excitation frequency. The excitation shift was always made away from the spectral window being viewed. The presence of Raman lines was indicated in the difference spectrum by features that approximated the derivative of a peak, whereas small changes in the shape of the fluorescence emission contributed a smooth background, which could be easily removed by subtraction of a polynomial fit. With or without a flat-field correction (see below), the difference of two emission spectra taken without a shift in excitation frequency was a shot-noise-limited flat line. All the difference data are shown without a flat-field correction. To obtain a Raman spectrum from a difference spectrum, we assumed that the Raman spectrum was a sum of Gaussian peaks, each with independent width, amplitude, and position. The number of peaks was determined by inspection of the difference spectra. Then, for a known shift of excitation frequency, the parameters of each Gaussian peak were determined by a nonlinear least-squares fit of the complete predicted difference spectrum to the difference data, and the resulting best-fit values were used to generate the Gaussian peaks of the simulated Raman spectrum. A more complete description of this technique and its capabilities will be presented elsewhere.

RESULTS

The usual technique for measuring Raman spectra of fluorescence samples is to collect the emission from the sample, divide the resulting signal by that obtained using a spectrally broad emission source such as a standard lamp (the flat-field correction), and, finally, subtract a polynomial fit to the fluorescence background to display the Raman peaks. In the present case, the Raman signals are $\approx 10^{-3}$ times the fluorescence background, and without prior knowledge of the peak positions, it is difficult to identify unambiguous Raman lines in the flat-field-corrected and background-subtracted spectrum. In fact, initial attempts to obtain resonance Raman spectra of RCs using this technique generated artifactual peaks that did not shift when the excitation frequency was changed. By contrast, the difference technique is sensitive to peaks that shift with the excitation frequency and so avoids artifacts resulting from the flat-field correction or background subtraction.

Typical difference spectra of RCs from *R. sphaeroides* (R-26) (with small backgrounds removed by a polynomial fit) are shown in Fig. 2. In Fig. 2 the results of identical experimental runs on the same sample before (curves B) and after (curves C) treatment with $K_3Fe(CN)_6$ are shown. The difference data were fit and the parameters obtained were used to generate "integrated" Raman spectra. The fits to the difference data are shown through the data, whereas the resulting conventional spectra are plotted above the data (curves A). With 850-nm excitation, Raman lines are seen at 94, 127, 202, 685, and 730 cm^{-1}. These features disappear when excess $K_3Fe(CN)_6$ is added, demonstrating that they all result from resonance enhancement by the special pair. With 810-nm excitation, the low-frequency region has Raman lines

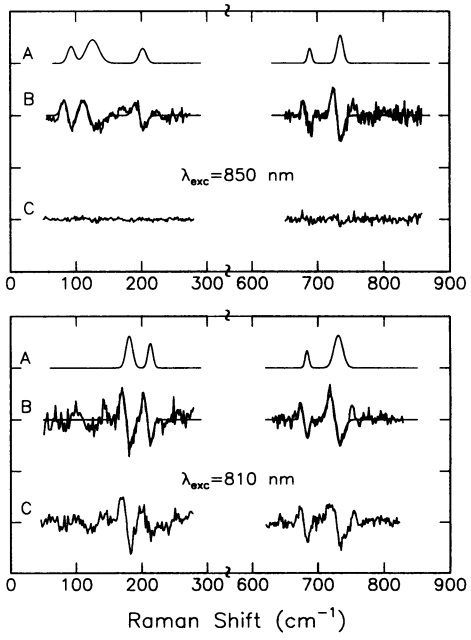

FIG. 2. Shifted excitation Raman difference spectra of *R. sphaeroides* (R-26) obtained with 850-nm excitation (exc) (*Upper*) and with 810-nm excitation (*Lower*). The middle curves (B) are the difference spectra obtained from unoxidized RCs, and the bottom curves (C) are those obtained from the same sample after treatment with $K_3Fe(CN)_6$. The low-frequency data with 850-nm excitation (upper left) are multiplied by two relative to all other data. The upper curves (A) are the simulated Raman spectra generated from the fits that are drawn through the difference data (curves B).

at 181 cm^{-1} and 213 cm^{-1}, while the 730 cm^{-1} and weaker 685 cm^{-1} lines are still observed. None of the features observed with 810-nm excitation are affected by treatment with $K_3Fe(CN)_6$, indicating that they do not result from resonance enhancement by P. The most likely source of the Raman intensity in these modes is enhancement from the strong 800-nm absorption in RCs, largely due to the monomeric Bchls, which is unchanged (except for a small wavelength shift) by treatment with $K_3Fe(CN)_6$ (see Fig. 1). The low-frequency anti-Stokes spectral region, examined with both 850-nm and 810-nm excitation (data not shown), has features identical to those seen in the low-frequency Stokes regions, and the anti-Stokes and Stokes features behave identically upon addition of $K_3Fe(CN)_6$. The oxidation experiments and the comparison of Stokes and anti-Stokes results with different excitation wavelengths confirm that, with 850-nm excitation, we are observing Raman scattering from P.

Both the low-frequency and 730 cm^{-1} spectral regions were examined at several excitation wavelengths with the difference technique; the results are shown in Fig. 3. These data have been scaled to compensate for variations in incident laser power and for monochromator and detector sensitivity. The important qualitative result is that resonant enhancement is observed throughout the low-energy P absorption band, providing additional evidence that the scattering observed with 850-nm excitation is dominated by P.

The difference spectra, the excitation profiles, and the experiments with the chemically oxidized RCs demonstrate the presence of resonance Raman scattering with excitation in the P absorption band. With these critical controls in hand, a more detailed examination of the scattering observed with 850-nm excitation is possible. First, a full difference spectrum, covering the region from 30 to 1760 cm^{-1}, was obtained and is shown, after correction for the instrument sensitivity, in Fig. 4 (bottom spectrum). The noise is quite large in the high-frequency region because of the rapid decline in detector sensitivity. The noise in this region precludes a fit to the data; however, no intense Raman lines are seen above 900 cm^{-1}. We emphasize that relatively weak high-frequency Raman lines may not have been observed because of the noise in that spectral region. For the data below 900 cm^{-1}, reproducible difference features were fit, and the resulting simulated Raman spectrum is shown (top spectrum). In addition to the peaks discussed thus far, modes are found at 36 cm^{-1}, 71 cm^{-1}, 337 cm^{-1}, and 898 cm^{-1}. The 36 cm^{-1} mode was difficult to fit because its Raman shift was so low that the peak

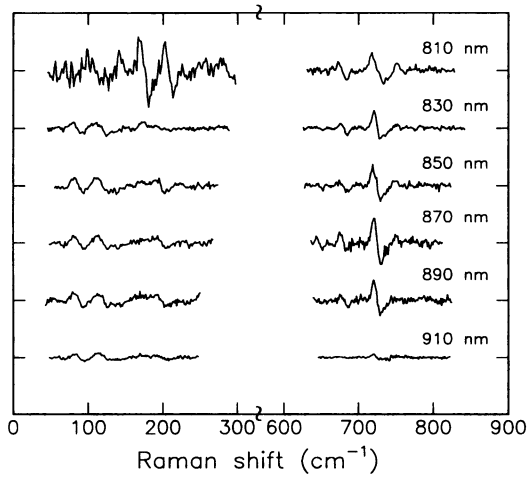

FIG. 3. Difference spectra of *R. sphaeroides* (R-26) obtained at different excitation wavelengths. Data in the low-frequency region (left) are multiplied by two relative to those in the high-frequency region (right), and the labels indicate the excitation wavelength for each curve (see Fig. 1).

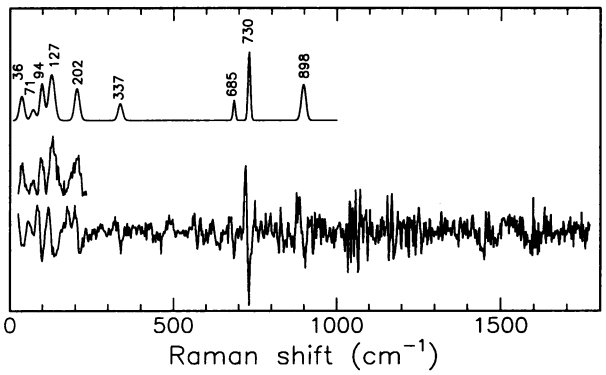

FIG. 4. Rapid-flow resonance Raman spectra of *R. sphaeroides* (R-26) RCs with 850-nm excitation. At bottom is the complete difference spectrum from 30 cm^{-1} to 1760 cm^{-1}. The high-frequency data are shown to demonstrate that no large Raman lines are present above 898 cm^{-1}. Small Raman features could be masked by the noise above 1000 cm^{-1}, and no attempt was made to fit the data in this region. The middle spectrum is a flat-field-corrected and background-subtracted spectrum that exposes the 36-cm^{-1} feature. At top is a simulated spectrum using the Gaussian parameters obtained by fitting reproducible features in the difference spectrum. The approximate relative intensities of the modes that were fit are 0.4, 0.2, 0.6, 1.0, 0.6, 0.3, 0.2, 0.7, and 0.7 for the 36, 71, 94, 127, 202, 337, 685, 730, and 898 cm^{-1} modes, respectively, with estimated uncertainties of ±25%. The 71-cm^{-1} mode may be an overtone peak of the strong 36-cm^{-1} mode.

moved out of the detection window when the excitation frequency was shifted, so the full difference feature could not be determined. However, this mode was verified to disappear when 30 mM $K_3Fe(CN)_6$ was added to the RCs and is not observed at all using 810-nm excitation. As an additional check, with an accumulation time of ≈2 hr, small, reproducible, low-wavenumber peaks in the flat-field-corrected data were identified after subtraction of a fit to the fluorescence (see middle spectrum). These peaks were all found to shift with excitation frequency. The agreement between the spectrum obtained from the difference technique and the flat-field corrected spectrum is quite good.

DISCUSSION

A resonance Raman study of RCs with near-IR excitation must overcome two principal difficulties. (*i*) Upon excitation of RCs, reversible photooxidation occurs and leads to a bleach of the P absorption. This problem is overcome by use of the rapid-flow technique, as has been demonstrated for resonance Raman studies of other chromophores that undergo efficient photochemistry (22). (*ii*) The Raman scattering must be distinguished from the fluorescence background. We overcome this problem by taking a difference of spectra obtained with slightly shifted excitation frequencies. The fluorescence background is removed, leaving difference features from the underlying Raman lines. The difference technique requires much less signal averaging to identify definitive Raman peaks than the traditional flat-field approach.

The Raman-active vibrations that we have examined extensively fall into three distinct classes. (*i*) There are those modes that are only observed when the excitation is resonant with the ^1P state. The frequencies of the strongest of these are 36 cm^{-1}, 94 cm^{-1}, 127 cm^{-1}, and 202 cm^{-1}. In addition to appearing only for excitation resonant with the P absorption, these modes disappear when the special pair is oxidized with $K_3Fe(CN)_6$. Because these modes are not observed when excitation is resonant with monomeric Bchl, they are either associated solely with P and are not intrinsic, intramolecular Bchl modes, or they are Bchl modes that are resonantly enhanced by the P absorption but not by the monomer

absorption. (*ii*) Modes of the second class are those that are observed only when the excitation is resonant with the monomer absorption band. The 181 cm^{-1} and 213 cm^{-1} modes excited at 810 nm are in this category. These modes are unaffected by treatment with the oxidant, so presumably they are associated with the Bchl monomer and are resonantly enhanced by its Q_y absorption band. (*iii*) The third category contains modes that are observed irrespective of whether the excitation wavelength is resonant with the monomer or the dimer absorption. These modes have frequencies of 685 cm^{-1} and 730 cm^{-1}. The response of these modes to $K_3Fe(CN)_6$ treatment depends upon the excitation wavelength. When the excitation is resonant with the ^1P state, the modes disappear in the oxidized RCs, but they are unaffected by oxidation if the excitation is resonant with the Bchl monomer absorption. The obvious interpretation is that these modes are intrinsic to Bchl monomers and, therefore, also appear in the Bchl dimer. Curiously, the modes with frequencies of 181 cm^{-1} and 213 cm^{-1}, which are seen with 810-nm excitation, appear to be modes of the Bchl monomer that are not enhanced in the dimer. However, these modes might overlap with and contribute to the dimer mode at 202 cm^{-1}. In fact, this dimer mode appears somewhat asymmetric, and the corresponding difference feature is difficult to fit well using our simple Gaussian model. At present, the quality of the data does not allow this issue to be resolved.

Previous Raman studies of RCs have used three general techniques. (*i*) Resonance Raman of RCs has been done by using excitation resonant with electronic states of higher energy than ^1P (26, 27). This technique avoids the problem of interfering fluorescence because the higher energy electronic states of RCs are quite short-lived. Although these studies are valuable for obtaining structural information about RCs, they provide no information about the Raman-active modes that are resonantly enhanced by the photochemically active state of the special pair. (*ii*) Another technique for Raman studies of RCs is Fourier transform (FT) Raman spectroscopy using 1064-nm excitation (28, 29). FT Raman studies might, in principle, provide information about modes that are resonantly enhanced by the P absorption band, but the lack of specific resonance enhancement complicates matters. Recently published FT Raman studies of RCs (28, 29) agree gratifyingly well with our resonance Raman data in the presence of modes at 730 cm^{-1} and 895 cm^{-1} and also show congested, broad features in the high wavenumber region (1400 cm^{-1}–1700 cm^{-1}). Unfortunately, the study of the important low-frequency scattering with FT Raman is technically difficult, and no FT Raman spectra of RCs have been published that cover the region below 200 cm^{-1}. (*iii*) The third experimental technique is resonance Raman of RCs by using excitation directly resonant with the near-IR, P absorption band. One such paper has been published before our work—low-frequency scattering spectra, obtained from a static sample at 12 K, are reported for RCs isolated from *R. sphaeroides* 2.4.1 (wild type) (30). Interestingly, the best signal-to-noise was obtained for excitation at 920 nm—that is, at the very red edge of the absorption band. At that excitation wavelength, very weak modes were observed at 102 cm^{-1} and 138 cm^{-1}, corresponding roughly to the modes we observe at 94 cm^{-1} and 127 cm^{-1}. However, the qualitative excitation profile for these low-frequency modes did not follow the absorption spectrum. In fact, no Raman scattering was observed with excitation near the peak of the absorption band. In contrast, our qualitative excitation profile data show resonant enhancement throughout the P absorption. Because Raman excitation profiles provide important information about the excited electronic state (19, 21, 31), the discrepancy is an important one. The experimental conditions used in the two studies might account for the difference—a low-temperature static sample is subject to photochemical bleaching, which will be most pronounced for excitation at the absorption peak, but the rapid-flow technique avoids this problem.

Resonance Raman data provide information that can be used in the quantitative interpretation of the extensive hole-burning studies of the lowest energy absorption band of RCs (9–17). In the hole-burning experiments, a spectrally broad hole is observed, and with burn frequencies on the red edge of the P absorption band, a much narrower, extremely weak zero-phonon hole is seen. One interpretation for these results is that the equilibrium nuclear position is displaced along low-frequency modes upon passage from the ground to the excited electronic state (13, 15, 17). With a model assuming only two displaced modes (17), the hole-burning and absorption data for *R. sphaeroides* are fit by modes with frequencies of 35 cm^{-1} and 125 cm^{-1}, and dimensionless displacements Δ corresponding to $S = 2.0$ and 1.5, respectively, where $S = \Delta^2/2$. However, even though the total S can be determined to be $\approx$3.5 (13, 17), the lack of structure in both the absorption spectrum and the phonon sideband of the hole spectrum precludes the unambiguous determination of excited-state displacements without independent knowledge of the number and frequencies of the displaced modes (13). For instance, it has also been shown that a three-mode model can fit the absorption and hole-burning data by using modes with frequency ranges of 20–50 cm^{-1}, 100–140 cm^{-1}, and 150–500 cm^{-1}, and corresponding S values of 1.7–2.6, 0.5–1.2, and 0.1–0.7 (13). Our work has determined the ground-state frequencies of the coupled modes. We find only a few modes, with ground-state frequencies of 36 cm^{-1}, 94 cm^{-1}, 127 cm^{-1}, 202 cm^{-1}, 730 cm^{-1}, and 898 cm^{-1}, that are strongly coupled to the optical transition, and the relative Raman intensities of these modes appear qualitatively consistent with the displacements used to model hole-burning and absorption data, if the Raman scattering occurs in the short-time limit where Raman intensity is proportional to $\omega^2 S$ (21). In addition, neither the hole-burning nor the absorption data can be reproduced by a model that includes high-frequency modes with large displacements, consistent with the lack of intense Raman modes in the high-frequency region. Thus, the resonance Raman data provide substantial support for interpretation of the hole-burning data as resulting from excitation of a manifold of displaced vibrations.

When the excitation is directly on resonance with the P absorption, only a few modes appear strongly in the resonance Raman spectra of RCs. This result is in striking contrast to Raman spectra of Bchl, or of RCs using excitation resonant with other electronic states, where a large number of modes, many with energies in the 1400–1700 cm^{-1} range, are Raman active (26–29, 32). Because the ^1P state of RCs is largely based on the Q_y states of the Bchl monomers that comprise P, the displaced modes in Bchl are likely to be displaced in ^1P. However, in monomeric chlorophylls, the Q_y transition is characterized by a small total displacement, with the most displaced modes having $S \approx 0.04$ (33). For ^1P, the total S is $\approx$3.5, and because this is distributed among only a few modes, the S of each of the observed modes is likely to be larger than for any monomeric Bchl mode. In other words, even though the large number of Raman-active modes observed in monomeric Bchl are probably also displaced in ^1P, they are not observed with the current signal-to-noise ratio. One possible explanation for large displacements in only a few modes is that, in general, electronic states with charge-transfer character demonstrate large nuclear displacements (see, for example, ref. 34). Thus, it is possible that the modes observed when on resonance with ^1P are those that are strongly affected by the charge-transfer character of ^1P, although the large intensity of the low-frequency modes seen with 810-nm excitation must also be considered.

The question of whether the Raman-active vibrations might be coupled to the primary electron transfer in RCs is an intriguing one. Simply put, this question is one of whether the modes that are displaced upon passage from P to ^1P include those that are displaced upon passage from ^1P to P^+. If the modes that are strongly displaced in ^1P gain their large values of S by coupling with the charge-transfer character in ^1P, then it is not unreasonable that one or more of these modes is further displaced in the fully charge-separated state P^+X^-, where X is the initial electron acceptor (B or H). Quantitative assignment of the normal coordinates corresponding to the observed Raman lines might also address this issue by examining whether the nuclear motions are those likely to be coupled to formation of P^+. The 730-cm^{-1} mode has been previously observed in Bchl and has been attributed to an in-plane C—N—C deformation (26). The low-frequency modes may involve motions of the metal (26), as well as in and out-of-plane deformations. All of these types of motions could certainly be strongly affected by a large change in charge density, but without specific mode assignments it is difficult to explain why only a few particular modes have large displacements. In addition to intramolecular modes, motion along the intra-dimer axis will almost certainly be coupled to changes in charge distribution. A semi-empirical calculation has suggested that the ground electronic state frequency of intra-dimer motion is $\approx$100 cm^{-1} (18), a frequency that corresponds well to either the 94-cm^{-1} or the 127-cm^{-1} modes that we observe. This speculation would be considerably more secure if the exact details of the charge-transfer character in ^1P and of the nuclear motions in the Raman-active vibrations were known, but it is provocative that the resonance Raman experiment may be probing those vibrational modes that are coupled to the primary charge separation in RCs.

SUMMARY AND PROSPECTS

We have observed resonance Raman scattering from isolated RCs of *R. sphaeroides* (R-26) using a shifted excitation difference technique and excitation in resonance with the lowest energy electronic state of P. Chemical oxidation experiments have shown that the resonance enhancement is from P when RCs are excited in the P absorption band, and the measurement of qualitative excitation profiles demonstrated that enhancement is observed throughout this absorption band. The frequencies and intensities of the observed resonance Raman-active modes are qualitatively consistent with previously published models of hole-burning results in RCs and provide the basis for a more quantitative interpretation of the absorption properties of P.

The ability to obtain well-characterized resonance Raman spectra of the photochemically active state of RCs will allow further exploration of RC photochemistry. The measurement and analysis of absolute Raman intensities will determine the displacements of vibrations and the time scale of vibrational or electronic damping in the excited state. Together with hole-burning results, this information should lead to a complete multimode model of the excited-state potential energy surface that can account for the low-temperature absorption spectrum and hole-burning data and the room-temperature absorption and resonance Raman data. A second important step will be the assignment of the vibrational modes of P. Bocian and coworkers (35, 36) have recently made important progress in the quantitative assignment of modes of a Bchl model compound, but the detailed assignment of low-frequency modes remains unresolved. In addition to model compound studies, mutant and isotopic studies may also assist the assignment of the vibrational modes of P. Mode assignments and a complete Raman intensity analysis will allow an examination of the coupling of vibrational and electronic motions in RCs and should provide a detailed experimentally based picture of the initial nuclear motions that occur in photosynthesis.

We thank Tom Middendorf and Martin Steffen for assistance and valuable discussions and Tom Wyatt for arranging the loan of the Ti-sapphire laser. For support of this work, R.A.M. thanks the National Science Foundation (CHE 86-15093), and S.G.B. gratefully acknowledges the National Science Foundation Biophysics Program. A.P.S. was supported by a National Institutes of Health postdoctoral fellowship (GM14298), and N.J.C. acknowledges the Henry Luce Foundation for support by a C. B. Luce Fellowship.

1. Deisenhofer, J. & Michel, H. (1989) *Science* **245**, 1463–1473.
2. Feher, G. (1989) *Annu. Rev. Biochem.* **58**, 607–663.
3. Friesner, R. A. & Won, Y. (1989) *Biochim. Biophys. Acta* **977**, 99–122.
4. Boxer, S. G., Goldstein, R. A., Lockhart, D. J., Middendorf, T. R. & Takiff, L. (1989) *J. Phys. Chem.* **93**, 8280–8294.
5. Lösche, M., Feher, G. & Okamura, M. Y. (1987) *Proc. Natl. Acad. Sci. USA* **84**, 7537–7541.
6. Lösche, M., Feher, G. & Okamura, M. Y. (1988) in *The Photosynthetic Bacterial Reaction Center—Structure and Dynamics*, eds. Breton, J. & Vermeglio, A. (Plenum, New York), pp. 151–164.
7. Lockhart, D. J. & Boxer, S. G. (1987) *Biochemistry* **26**, 664–668, 2958.
8. Lockhart, D. J. & Boxer, S. G. (1988) *Proc. Natl. Acad. Sci. USA* **85**, 107–111.
9. Meech, S. R., Hoff, A. J. & Wiersma, D. A. (1985) *Chem. Phys. Lett.* **121**, 287–292.
10. Meech, S. R., Hoff, A. J. & Wiersma, D. A. (1986) *Proc. Natl. Acad. Sci. USA* **83**, 9464–9468.
11. Boxer, S. G., Middendorf, T. R. & Lockhart, D. J. (1986) *FEBS Lett.* **200**, 237–241.
12. Boxer, S. G., Lockhart, D. J. & Middendorf, T. R. (1986) *Chem. Phys. Lett.* **123**, 476–482.
13. Middendorf, T., Mazzola, L., Gaul, D., Schenck, C. & Boxer, S. (1991) *J. Phys. Chem.*, in press.
14. Hayes, J. M. & Small, G. J. (1986) *J. Phys. Chem.* **90**, 4928–4931.
15. Hayes, J. M., Gillie, J. K., Tang, D. & Small, G. J. (1988) *Biochim. Biophys. Acta* **932**, 287–305.
16. Tang, D., Jankowiak, R., Gillie, J. K., Small, G. J. & Tiede, D. M. (1988) *J. Phys. Chem.* **92**, 4012–4015.
17. Johnson, S. G., Tang, D., Jankowiak, R., Hayes, J. M., Small, G. J. & Tiede, D. M. (1989) *J. Phys. Chem.* **93**, 5953–5957.
18. Warshel, A. (1980) *Proc. Natl. Acad. Sci. USA* **77**, 3105–3109.
19. Won, Y. & Friesner, R. A. (1987) *Proc. Natl. Acad. Sci. USA* **84**, 5511–5515.
20. Won, Y. & Friesner, R. A. (1988) *J. Phys. Chem.* **92**, 2214–2219.
21. Myers, A. B. & Mathies, R. A. (1987) in *Resonance Raman Spectra of Polyenes and Aromatics*, Biological Applications of Raman Spectrometry, ed. Spiro, T. G. (Wiley, New York), Vol. 2, pp. 1–58.
22. Mathies, R., Oseroff, A. R. & Stryer, L. (1976) *Proc. Natl. Acad. Sci. USA* **73**, 1–5.
23. Zankel, K., Reed, D. & Clayton, R. (1968) *Proc. Natl. Acad. Sci. USA* **61**, 1243–1249.
24. Schenck, C. C., Blankenship, R. E. & Parson, W. W. (1982) *Biochim. Biophys. Acta* **680**, 44–59.
25. Okamura, M., Isaacson, R. & Feher, G. (1975) *Proc. Natl. Acad. Sci. USA* **72**, 3491–3495.
26. Lutz, M. & Mäntele, W. (1991) in *Chlorophylls*, ed. Scheer, H. (CRC, Boca Raton, FL), pp. 855–902.
27. Robert, B. (1990) *Biochim. Biophys. Acta* **1017**, 99–111.
28. Johnson, C. K. & Rubinovitz, R. (1990) *Appl. Spectrosc.* **44**, 1103–1106.
29. Mattioli, T. A., Hoffmann, A., Robert, B., Schrader, B. & Lutz, M. (1991) *Biochemistry* **30**, 4648–4654.
30. Donohoe, R. J., Dyer, R. B., Swanson, B. I., Violette, C. A., Frank, H. A. & Bocian, D. F. (1990) *J. Am. Chem. Soc.* **112**, 6716–6718.
31. Warshel, A. (1977) *Annu. Rev. Biophys. Bioeng.* **6**, 273–300.
32. Bocian, D. F., Boldt, N. J., Chadwick, B. W. & Frank, H. A. (1987) *FEBS Lett.* **214**, 92–96.
33. Gillie, J. K., Small, G. J. & Golbeck, J. H. (1989) *J. Phys. Chem.* **93**, 1620–1627.
34. Brillante, A. & Philpott, M. R. (1980) *J. Chem. Phys.* **72**, 4019–4030.
35. Schick, G. A. & Bocian, D. F. (1987) *Biochim. Biophys. Acta* **895**, 127–154.
36. Donohoe, R. J., Frank, H. A. & Bocian, D. F. (1988) *Photochem. Photobiol.* **48**, 531–537.